Biochemical Pharmacology 91 (2014) 181–190

Contents lists available at ScienceDirect

Biochemical Pharmacology

journal homepage: www.elsevier.com/locate/biochempharm

Dissecting histone deacetylase role in pulmonary arterial smooth muscle cell proliferation and migration

Margherita Galletti [a,b,1], Silvia Cantoni [a,b,1,*], Filippo Zambelli [a,c], Sabrina Valente [b], Massimiliano Palazzini [b], Alessandra Manes [b], Gianandrea Pasquinelli [b], Antonello Mai [d], Nazzareno Galiè [a,b], Carlo Ventura [a,e]

[a] National Institute of Biostructures and Biosystems (NIBB), University of Bologna, Bologna, Italy
[b] Department of Experimental, Diagnostic and Specialty Medicine (DIMES), University of Bologna, Bologna, Italy
[c] Società Italiana Studi Medicina della Riproduzione (S.I.S.Me.R.), Reproductive Medicine Unit, Bologna, Italy
[d] Department of Drug Chemistry & Technologies, Sapienza University of Rome, Rome, Italy
[e] Stem Wave Institute for Tissue Healing (SWITH), Gruppo Villa Maria (GVM) and Ettore Sansavini Health Foundation – ONLUS, Lugo, Ravenna, Italy

ARTICLE INFO

Article history:
Received 24 April 2014
Accepted 15 July 2014
Available online 22 July 2014

Keywords:
Pulmonary hypertension
Histone deacetylase
Proliferation
Migration
Smooth muscle cells

Chemical compounds studied in this article: MC1855 (PubChem CID: 49769450); Sodium butyrate (PubChem CID: 5222465); 4-(dimethylamino)-N-[6-(hydroxyamino)-6-oxohexyl]-benzamide (PubChem CID: 3811); Calyculin A (PubChem CID: 5311365).

ABSTRACT

Pulmonary Arterial Hypertension (PAH) is a rare and devasting condition characterized by elevated pulmonary vascular resistance and pulmonary artery pressure leading to right-heart failure and premature death.

Pathologic alterations in proliferation, migration and survival of all cell types composing the vascular tissue play a key role in the occlusion of the vascular lumen. In the current study, we initially investigated the action of selective class I and class II HDAC inhibitors on the proliferation and migration of pulmonary artery smooth muscle cells (PASMCs) after exposure to Platelet Derived Growth Factor (PDGF). Class I HDAC inhibitors were able to counteract the hyperproliferative response to PDGF, reducing both proliferation and migration in PASMCs, while class II were ineffective. Selective silencing with siRNAs targeted against different HDACs revealed a major role of class I, and within this class, of HDAC1 in mediating PDGF-induced Akt Phosphorylation and Cyclin D1 (CycD1) expression. These results from these combinatorial approaches were further confirmed by the ability of a specific HDAC1 inhibitor to antagonize the PDGF action. The finding that HDAC1 is a major conductor of PDGF-induced patterning in PAH-PASMCs prompts the development of novel selective inhibitors of this member of class I HDACs as a potential tool to control lung vascular homeostasis in PAH.

1. Introduction

Pulmonary Arterial Hypertension (PAH) is a rare and multifactorial condition characterized by elevated pulmonary vascular resistance and pulmonary artery pressure leading to right-heart failure and premature death [1,2].

The progressive increase of pressure load is due to a dramatic pulmonary arterial wall remodeling involving all cellular components of the vessel. Dysfunction in cell proliferation, migration, survival, inflammation and thrombosis lead to a thickening of the vascular walls and to a subsequent occlusion of the lumen [3]. Within many factors involved in these processes, platelet derived growth factor (PDGF) pathway plays a pivotal role in modulating Pulmonary Artery Smooth Muscle Cells (PASMCs) proliferation and migration [4,5].

Current treatments are only able to slow down the progression of PAH thus a real cure does not exist [6]. Furthermore, the mechanisms underlying the onset and progression of PAH have not been fully elucidated yet. For these reasons studies addressing the etiology of the disease and directed to identify new therapeutic targets are needed.

Histone Deacetylases (HDACs) remove the acetyl group from the amino termini of Lysine residues of histones and other various substrates including transcription factors, chaperones, as well as

* Corresponding author at: Laboratory of Experimental Cardiology, Pav.21 DIMES University of Bologna, Via Massarenti 9, 40138 Bologna, Italy.
Tel.: +39 0516363605; fax: +39 051344859.
E-mail address: silcant@gmail.com (S. Cantoni).
[1] These authors contributed equally to this work.

http://dx.doi.org/10.1016/j.bcp.2014.07.011

many regulators involved in DNA repair, cell signaling or metabolism [7]. Within 18 mammalian family members the 11 known zinc-dependent HDACs are classified into 4 subgroups: class I (HDAC 1, 2, 3, 8), class IIa (HDAC 4, 5, 7, 9), class IIb (HDAC 6, 10) and class IV (HDAC 11) [8,9].

These enzymes are involved in many different biological and pathological processes: their role in cancer progression has long been established since 1998 [10] but these molecules have been associated also with Pulmonary Arterial Hypertension [11], diabetes [12], memory formation [13], Parkinson disease [14] and inflammation processes in Rheumatoid Arthritis [15]. Histone Deacetylase inhibitors (HDACis) have been developed to counteract the proliferation of cancer cells and showed promising results by inducing cell cycle arrest, apoptosis and anti-angiogenic effects [16]. Pan-HDACis also reduce cardiac hypertrophy in PAH rats and inhibit the "highly proliferative phenotype" of PDGF-treated vascular cells [11]; selective class I HDACis counteract hypoxia-induced cardiopulmonary remodeling in rats [17] and class II HDACis are involved in blocking the fetal gene reactivation in heart, reducing hypertrophy [18]. Among different classes, however, it is still not clear which specific HDAC is involved in promoting these pathological processes. In PAH abnormalities are found in both heart and lung cells. The need for "more" specific targets also arises from the fact that different HDACs among their class I have been reported to have distinct functions in heart and lungs: it is known indeed that the inhibition of class I HDAC reduces cardiopulmonary vessel remodeling, but the knockout of HDAC3 (belonging to class I) induces a hypertrophic phenotype in hearts [19].

We previously provide evidence that a pan-inhibitor of HDACs, Sodium Butyrate (NaBU), reduced the proliferation and migration induced by PDGF in PASMCs isolated from rats with monocrotaline (MCT)-induced PAH [20].

In the current study, we aimed at further dissecting the role of HDACs in these cells, and attempted to establish whether the proliferative/migratory action of PDGF may be executed through the intervention of multiple classes of HDACs, including class I and II, or it may conversely involve a single HDAC class, and in the affirmative, a targeted class member. For this purpose, we used a combinatorial approach encompassing the use of two novel hydroxamate derivatives MC1855 [21] and MC1575 [8], displaying specific inhibitory action toward class I and II HDACs, respectively, as well as the use of a specific inhibitor of class I HADC1. With this strategy, and by the aid of siRNAs specifically directed against each member of class I HDAC, we provide evidence that the PDGF effects on PAH PASMCs were primarily elicited through the activity of class I HDAC1.

2. Methods

2.1. Ethics statement

Animal use was approved by the Bioethics Committee of the University of Bologna, in compliance with Directive 2010/63/EU of the European Parliament. The study was conducted adhering to the institutions guidelines for animal husbandry regarding food space light temperature (23–25 °C).

2.2. Cell isolation and culture conditions

Adult male Sprague-Dawley rats (200–250 g in body weight; Harlan Laboratories; Indianapolis, IN, USA) were subjected to a subcutaneous injection of 60 mg/kg of MCT (Sigma–Aldrich; St. Louis, MO, USA) [20]. After 28 days, all rats were anesthetized in a CO_2/O_2 mixture and subsequently killed by cervical dislocation. Intrapulmonary arteries were isolated and cleaned of connective tissue. The isolation of PASMCs, from PAH-animals, has been performed using a modification of previously described method [22]. The tissue was digested at 37 °C for 20 min in DMEM containing collagenase type I, 250 U/ml (Sigma–Aldrich; St. Louis, MO, USA). Fetal Bovine Serum (FBS) 10% was added to stop the reaction and the digested pieces were placed into petri dish containing fresh complete medium. After reaching confluence cells were frozen. PASMCs were cultured in DMEM with 10% FBS, 100 U/ml penicillin and 100 μg/ml streptomycin, 4 mM L-glutamine (all reagents from LONZA; Basel, Switzerland). PASMCs from the third to the fourth passages were used for all studies. To induce cell cycle synchronization a serum starvation was performed culturing cells at low percentage of serum (0.5% FBS) for 24 h. PASMCs were induced to proliferate and migrate by replacing starvation medium with fresh low serum medium containing 20 ng/ml PDGF (PeProtech; Rocky Hill, NJ, USA). MC1855 and MC1575 were synthesized in our laboratories at Sapienza University of Rome (Rome, Italy) as previously described [23], dissolved in DMSO and stored at −20 °C before use. NaBU and 4-(dimethylamino)-N-[6-(hydroxy amino)-6-oxohexyl]-benzamide (HDAC1-I) were purchased from Sigma–Aldrich (St. Louis, MO, USA) and Santa Cruz Inc. (Santa Cruz, CA, USA), respectively. The HDACis were added at the indicated concentrations concurrently with the PDGF, while the phosphatase inhibitor Calyculin A (CA), (Sigma–Aldrich; St. Louis, MO, USA), were administered 1 μM 1 h before the treatment. All experiments were repeated at least five times, unless otherwise mentioned.

2.3. MTT assay

PASMCs were seeded 3000 cells/cm^2 in 48-well plates and starved for 24 h. After 24 h of treatment MTT assay (Sigma–Aldrich; St. Louis, MO, USA) was performed to test cell growth. Cells were then incubated with MTT (20 μl/well of 5 mg/ml 3-(4,5-dimethylthiazol-2-yl)-2,5-diphenyltetrazolium bromide in phosphate buffered saline [PBS]) for 3 h and lysed with the same volume of lysis buffer (10% SDS 10 mM NaOH), the absorbance was measured at 570 nm with a spectrophotometric plate reader.

2.4. Measurement of cell migration in vitro

Cells were seeded (15,000 cells/well in 24-well plates), starved for 24 h and cultured with treating medium for additional 16 h. The confluent cell monolayer was scraped with a pipette tip across the diameter of the well. After removal of cell debris by washing with PBS two times, cells were observed for 6 h. The wound area at the beginning of wounding and at the end of treatment was photographed respectively under an inverted phase-contrast microscope equipped with digital sight camera (Nikon; Tokio, Japan). The recovered surface area was calculated by subtracting the wound area at the end of treatment from the corresponding original wound area.

2.5. Immunofluorescence

Cycling cells expressing ki67 protein were identified using a single immunofluorescence staining. PASMCs were seeded on glass slides into 12-well plates at a density of 3000 cells/cm^2, starved and treated with the appropriate molecules in low-serum medium. After 24 h, cells were washed, fixed in 2% paraformaldehyde in PBS for 4 min at room temperature (RT) and permeabilized with 0.5% Tryton X-100 for 10 min After washes, the slides were treated with 1% bovine serum albumin (BSA), (Sigma–Aldrich; St. Louis, MO, USA) in PBS solution for 30 min at RT in a wet chamber to reduce non-specific staining and stained for 1 h at 37 °C with monoclonal antibody anti-ki67 (1:100, Novocastra, Leica Microsystems;

Wetzlar, Germany). After washing, the slides were labeled with AlexaFluor-488 (1:250, Life Technology; Carlsbad, CA, USA) secondary antibody for 1 h at 37 °C in the dark. Both antibodies were diluted in 1% BSA in PBS. Samples were counterstained with Pro Long anti-fade reagent with DAPI (Molecular Probes, Thermo Fisher Scientific; Waltham, MA, USA) and observed in a Leica DMI6000 B inverted fluorescence microscope (Leica Microsystems; Wetzlar, Germany); all images were taken at 10× magnification. For negative control, samples were processed omitting the primary antibody.

2.6. AgNOR

Proteins associated with the nucleolar organizer regions were evaluated with AgNOR staining as previously described [24]. PASMCs seeded on glass slides were fixed with 2% paraformaldehyde in PBS plus 1% Triton X-100 for 10 min at RT. After washings, samples were stained with a solution containing one volume of 2% gelatin in 1% aqueous formic acid and two volumes of 50% silver nitrate for 10 min at 37 °C in the dark. Finally, PASMCs were dehydrated and mounted without nuclear contrast. Images were taken at 40× magnification through a video camera (JVC 3CCD video camera, KY-F55B) connected with a Leitz Diaplan light microscope; AgNOR analysis and quantification was carried out with Image-Pro Plus (Media Cybernetics, www.mediacy.com). AgNOR staining was measured in a minimum of 100 nuclei at 40× magnification; results were expressed as mean nucleolus (na)/nucleus (Na) ratio normalized to control.

2.7. Tunel assay

DNA fragmentation was evaluated with TUNEL (Terminal deoxynucleotidyl transferase-mediated dUTP Nick End-Labeling) assay using the "In situ cell death detection kit, POD" (Roche; Basel, Switzerland) following the manufacturer's instructions. Three μm-thick sections from formalin-fixed, paraffin-embedded PASMC pellets were dewaxed and rehydrated. Endogenous peroxidase was blocked by incubation in 3% H_2O_2 in methanol for 10 min at RT in the dark and antigenicity was recovered treating the samples with Proteinase K (DakoCytomation; Carpinteria, CA, USA) for 30 min at 37 °C. After washing, slides were treated with 50 μl of TUNEL reaction mixture (enzyme solution, diluted 1:5 in TUNEL Dilution Buffer and Label Solution) for 1 h a 37 °C in the dark. After that, sections were washed, incubated with Converted POD, revealed with DAB (3,3′-diaminobenzidine) (Sigma–Aldrich; St. Louis, MO, USA), counterstained with hematoxylin and mounted in a synthetic medium. As positive controls sections were treated with DNase I for 10 min at RT before exposure to TUNEL reaction mixture. Negative controls were obtained by omitting enzyme solution.

2.8. Pulmonary artery ring assay

Forty-eight-well plate were covered with Basement Membrane Extract (BME) (Trevigen; Gaithersburg, MD, USA) 100 μl/well and incubated for 30 min at 37 °C with 5% CO_2 to form semisolid medium. After sacrifice of rats intrapulmonary arteries were isolated, cleaned of fibroadipose tissue and cut into 1–1.5 mm long cross sections. Sections were rinsed five times using 0.5% FBS culture medium containing PDGF with or without HDACis and placed in 100 μl BME-coated 48-wells, then covered with an additional 100 μl of BME. During the experiment medium was replaced every three days.

2.9. Protein isolation, Western blotting

PASMCs monolayers were lysed in radioimmune precipitation assay buffer (RIPA) (Pierce; Thermo Fisher Scientific; Waltham, MA, USA). Protein content was determined using Bradford colorimetric protein assay (Sigma–Aldrich; St. Louis, MO, USA) following manufacturer's instructions. 30 μg of proteins were separated using 8–12% SDS-PAGE and transferred to a polyvinylidene difluoride membrane (Sigma–Aldrich; St. Louis, MO, USA). The filters were hybridized with the appropriate primary antibodies followed by a horseradish peroxidase-conjugated secondary antibody. The bands were visualized using the ECL method (Thermo Fisher Scientific; Waltham, MA, USA) and quantified using Molecular Imager® ChemiDoc™ XRS+ with

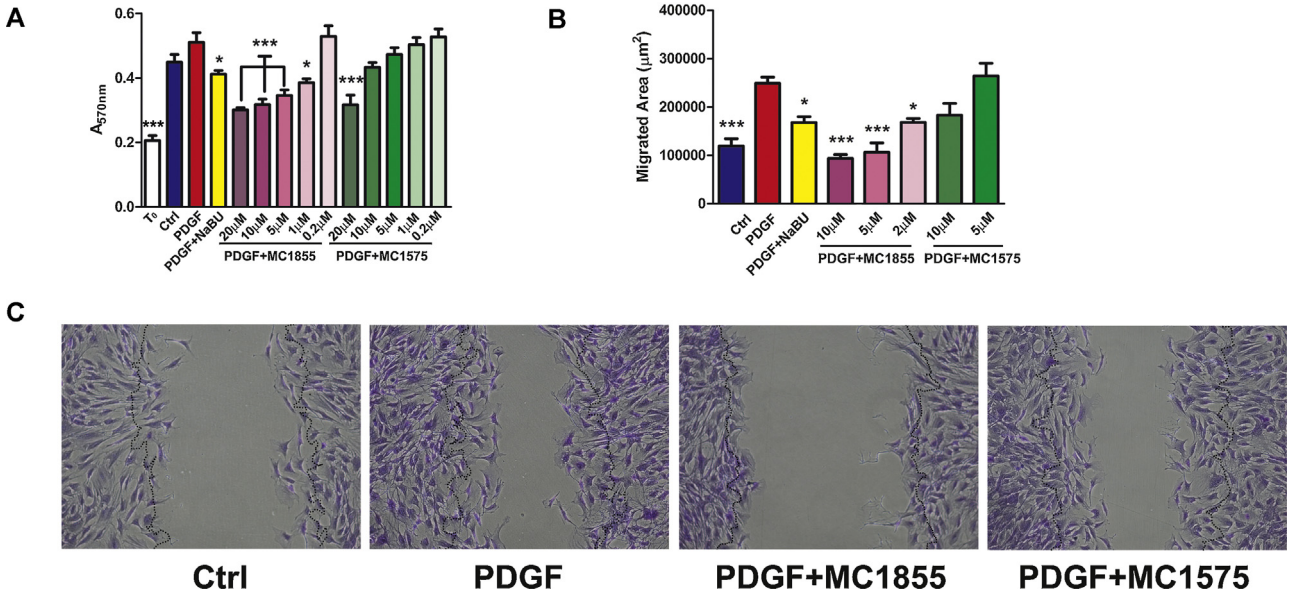

Fig. 1. Effect of MC1855 (class I specific HDACi) and MC1575 (class II specific HDACi) on PDGF-induced PASMCs proliferation and migration. (A) Effect of different doses of MC1855 or MC1575 on PDGF-induced proliferation as evaluated by MTT assay after 24 h of treatment. Time 0 (white lane) are also shown as a proliferation control. (B) Effect of different doses of MC1855 or MC1575 on PDGF-induced migration extent, measured as the difference in cells covered area after 6 h of observation. (C) Representative images from wound healing test (5 μM MC1855 and 5 μM MC1575). Dotted lines comprise cell covered area before the observation start. The quantitative results are expressed as mean ± sem and represent data averaged from 5 independent experiments $^{*}p < 0.05$; $^{**}p < 0.01$; $^{***}p < 0.005$ vs PDGF-treated group.

ImageLab™ Software (Bio-Rad Laboratories; Inc., Hercules, CA, USA). An anti-Vinculin antibody (1:5000, Sigma–Aldrich; St. Louis, MO, USA) was used as the loading control. The following antibodies were used: anti-Phospho Akt (Ser473) and anti-Akt (1:1000, Cell Signaling; Danvers, MA, USA), anti-CycD1 (1:1000, BD).

2.10. Quantitative RT-PCR

RNeasy Micro Kit (Qiagen) was utilized for RNA isolation from PASMCs. The cDNA was synthesized in a 20-μl reaction starting from 1 μg of total RNA with SuperScript III RT (Life Technologies; Thermo Fisher Scientific; Waltham, MA, USA). Quantitative RT-PCR was performed using the LightCyclerSYBR Green fast start kit (Lightcycler® FastStart DNA MasterPLUS SYBR Green I). The following Qiagen QuantiTect primers were used for real-time RT-PCR: ccnd1, hdac1, hdac2, hdac3, hdac8. Data were normalized using gapdh and actin b (actb) both from Qiagen (Hilden, Germany). For each primer a melting curve analysis was performed and real-time PCR efficiency was calculated. Results were analyzed and related plots were created using Relative Expression Software Tool (REST 2009 V2.0.13, Qiagen).

2.11. SiRNA transfection

The day before transfection, cells were seeded at the concentration of 10,000 cells/cm^2 into 6-well plates. LIPOFECTAMINE 2000 (Life Technology; Carlsbad, CA, USA) was used to transfect 10 nM siRNAs into the cells following manufacturer's instructions. The following siRNAs were used: rat HDAC1 HDAC2, HDAC3, HDAC8 iBONI siRNA pool were purchased from Riboxx (Dresden, Germany). After 24 h cells were starved, then treated for Western blotting analysis. Each HDAC level was evaluated by quantitative real-time PCR 48 h after the transfection in untreated starved cells.

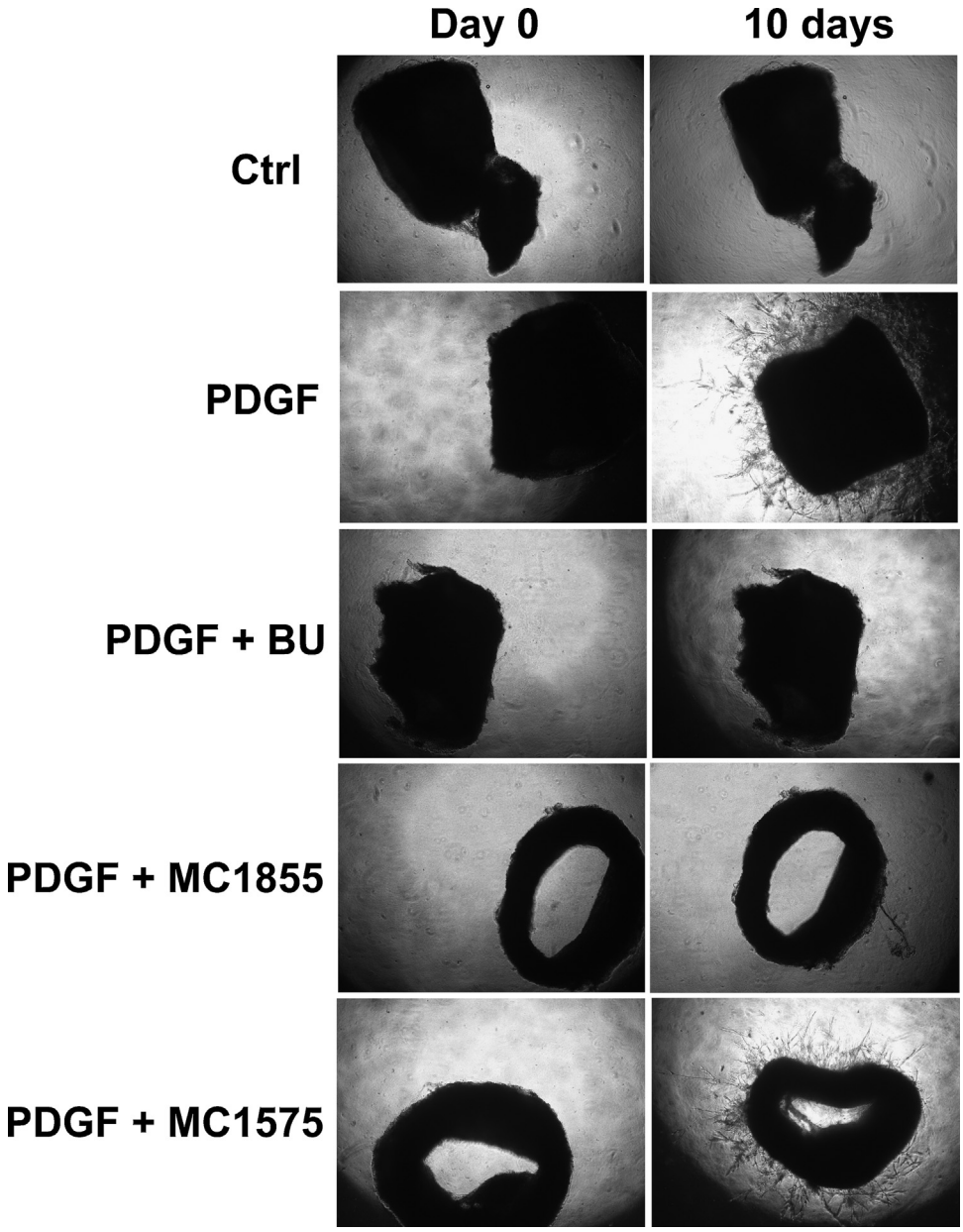

Fig. 2. Effect of 5 μM MC1855 (class I specific HDACi), 5 μM MC1575 (class II specific HDACi) and 5 mM NaBU (non-selective HDACi) on PDGF-induced sprouting in pulmonary artery rings from MCT-treated rats. Representative images of pulmonary artery before and after 10 days of treatment.

2.12. Statistical analysis

All values are expressed as the mean ± SEM. Data were statistically analyzed using one way ANOVA followed by appropriate post hoc test. All experiments were repeated at least five times, unless otherwise mentioned. A value for $p \leq 0.05$ was considered to be statistically significant.

3. Results

3.1. Class I, but not class II HDAC inhibitors counteract PDGF induced proliferation and migration of PASMCs from PAH-rats

We previously tested the ability of PDGF in inducing the proliferation of PASMCs isolated from rats with experimentally induced PAH and we demonstrated that NaBU, a broad-spectrum HDACi, counteracted the PDGF effect [20].

Here we show that increasing concentrations of a selective class I HDACi, MC1855 (ranging from 1 to 20 μM) significantly inhibited PASMC proliferation as revealed by MTT analysis after 24 h. On the contrary, the class II HDACi, MC1575, counteracted PDGF significantly only at the higher concentration (20 μM) (Fig. 1A).

Similar results were obtained when the effect of HDAC class selective inhibitors on PASMC migration was investigated using a wound healing assay. After 16 h of PDGF stimulation with or without HDACi treatment a wound was performed on the cells layer and the migration area was calculated after 6 h to exclude any confounding effect due to proliferation process. Remarkably, MC1855 dose-dependently inhibited the PDGF-induced migration whereas MC1575 did not affect the stimulatory effect of the growth factor even at the highest concentration (Fig. 1B and C).

To confirm the inhibitory effect of MC1855 on PDGF-induced migration, we performed pulmonary artery ring assay. Starting from 6 days of treatment and throughout a period of 12 days, PDGF induced sprouting in pulmonary artery rings from PAH-rats. MC1855, but not MC1575, was able to mitigate this effect, in an extent comparable to that achieved using the broad-spectrum HDACi, NaBU (Fig. 2).

3.2. MC1855, but not MC1575 down-regulate Cyclin D1 gene expression and accelerated Akt de-phosphorylation

In order to provide deeper insights into the molecular mechanisms of MC1855 we analyzed the Akt phosphorylation on Ser473. PDGF treatment was able to fully activate the Akt in PAH-Rat PASMCs. After 7 h, 5 μM MC1855 retraced the action of NaBU in decreasing Akt phosphorylation induced by a single PDGF administration (Fig. 3A). Interestingly, the inhibition of class II HDACs did not affect the phosphorylation state of Akt during the 24 h-treatment.

We next analyzed the activation of CycD1 one of the downstream components of PDGF signaling [25,26]. Gene expression of CycD1 was reduced in presence of MC1855 and NaBU but not with MC1575 (Fig. 3B), suggesting that class I HDACi are also able to act on the regulation on the CycD1.

Given the antiproliferative and antimigratory effects of MC1855, we decided to focus only on this molecule exclusively to establish possible mechanisms that class I HDACi may have on PAH cell proliferation and migration.

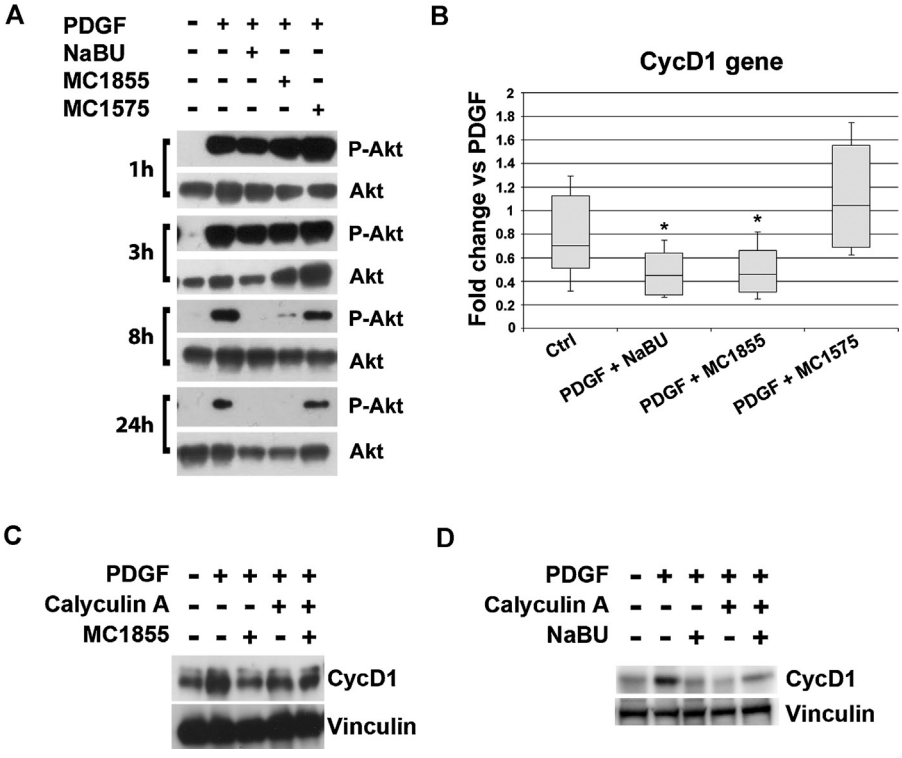

Fig. 3. Effect of MC1855 (class I specific HDACi) and MC1575 (class II specific HDACi) on Akt phosphorylation and CycD1 expression. (A) Phosphorylation state of Ser473-Akt in PASMCs after a treatment up to 24 h long with PDGF with or without 5 μM MC1855, 5 μM MC1575 or 5 mM NaBU (pan-inhibitor of HDACs). Untreated cells were used as a control (ctrl). Representative images of 5 different experiments. (B) Transcriptional level of CycD1 in PASMC after 7 h of PDGF-treatment with or without 5 μM MC1855, 5 μM MC1575 or 5 mM NaBU. Real-time PCR data, normalized to gapdh and actin beta housekeeping genes, were expressed as relative fold change of PDGF + HDACi compared to PDGF alone. Statistical analysis of 5 different experiments was analyzed using REST 2009 software (QIAGEN): $^{*}p < 0.05$. (C) Protein level after 7 h PDGF-treatment with or without MC1855 and/or phosphatase inhibitor Calyculin A (CA). Cells were pretreated with CA for 1 h before adding PDGF and HDACi. Untreated cells were used as a control. Representative image of 4 different experiments. (D) Protein level after 7 h PDGF-treatment with or without NaBU and/or phosphatase inhibitor CA. Cells were pretreated with CA for 1 h before adding PDGF and HDACi. Untreated cells were used as a control. Representative image of 3 different experiments.

3.3. MC1855 effects on Cyclin D1 expression through its action on phosphatases

We recently demonstrated that NaBU exerts its role on Akt phosphorylation acting on a phosphatase that is sensitive to phosphatase inhibitor Calyculin A (CA) after 7 h of treatment in presence of PDGF [20]. Interestingly, both MC1855 (Fig. 3C) and NaBU (Fig. 3D) blunted the CycD1 protein expression induced by PDGF, whereas the CA administration was able to restore CycD1 protein level (Fig. 3C and D).

3.4. HDAC1 is the key of MC1855 effect on Akt phosphorylation and Cyclin D1 expression

To identify the contribution on Akt phosphorylation of different HDACs belonging to class I, cells were transfected with specific siRNA for each of them: HDAC1, HDAC2, HDAC3 and HDAC8. As seen in RT-PCR (Fig. 4A), all HDACs belonging to class I were downregulated from 50% to 80% due to the specific siRNA effect. In addition, no effect on the other class I HDAC level was highlighted in HDAC1 siRNA transfected cells (data not shown).

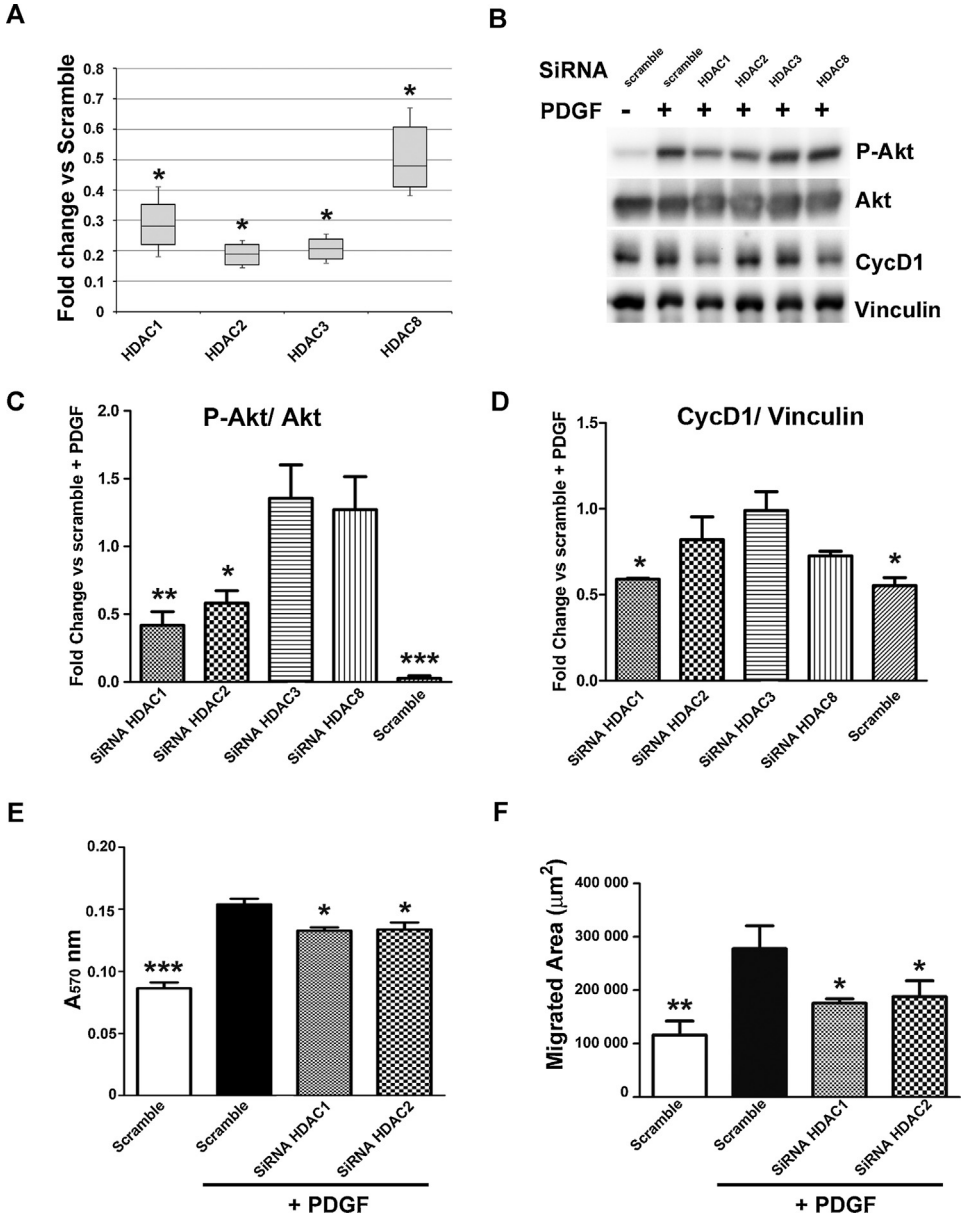

Fig. 4. Effect of separate class I HDACs knockdowns on Akt phosphorylation and CycD1 expression. (A) Relative quantification of mRNA expression levels in PASMCs after 48 h exposure to HDAC specific siRNAs. Fold changes compared to the scramble control were expressed as mean ± sem; $^{*}p < 0.05$, $^{**}p < 0.01$. (B) Effect of 48 h exposure to HDAC specific small interfering RNAs (siRNAs) on PDGF induced Ser473-phosphorylation of Akt and CycD1 levels increase after a 7-h treatment in PASMC. Total Akt and Vinculin were the internal loading controls respectively of Akt phosphorylation and CycD1 level. Representative images of 3 different experiments. (C) Effect on phosphorylated Akt as assessed by a densitometric analysis of Western blot experiments. Results were expressed as phospho/total Akt level change compared to that of the scramble control. Relative quantification of protein level was shown as mean ± sem; $^{*}p < 0.05$. (D) Effect on CycD1 level as assessed by a densitometric analysis of Western blot experiments. Results were expressed as CycD1/Vinculin level change compared to that of the scramble control. Relative protein level quantification was shown as mean ± sem; $^{*}p < 0.05$, $^{**}p < 0.01$. (E) Effect of siRNA against HDAC1 or HDAC2 on PDGF-induced proliferation as evaluated by MTT assay after 24 h of treatment. Data compared to the scramble + PDGF were expressed as mean ± sem; $^{*}p < 0.05$. (F) Effect of siRNA against HDAC1 or HDAC2 on PDGF-induced migration extent, measured as the difference in cells covered area after 6 h of observation. Data compared to the scramble + PDGF were expressed as mean ± sem; $^{*}p < 0.05$.

At 7 h, a time point at which MC1855 elicited significant downregulation of Akt phosphorylation, only HDAC1 and HDAC2 siRNA significantly reduced PDGF stimulation, while HDAC3 and HDAC8 siRNA had no appreciable effect when compared to scramble with addition of PDGF (Fig. 4B and C). Moreover, only HDAC1 siRNA reduced significantly PDGF-induced CycD1 protein expression (Fig. 4B and D). Interestingly, both HDAC1 and HDAC2 silencing caused reduction of proliferation (Fig. 4E) and migration (Fig. 4F) after 24 h and 6 h of treatment with PDGF, respectively.

3.5. A selective HDAC1 inhibitor efficiently mimics the effect of MC1855 on proliferation and migration

To further demonstrate that HDAC1 was the key effector of HDACi on PASMCs migration and proliferation, HDAC1-I, a commercial HDAC1 specific inhibitor [27,28] was utilized.

Starved cells were treated with PDGF in the presence or absence of 5 μM MC1855 or HDAC1-I at different concentrations ranging from 0.2 to 50 μM.

As shown in Fig. 5, HDAC1-I reduced PASMC proliferation, measured by MTT assay, in a dose-dependent manner from 2 to 50 μM without reducing the number of plated cells (Fig. 5A). Remarkably, HDAC1-I showed a similar effect on proliferation when used at the same concentration (5 μM) of MC1855 (Fig. 5A). A matching effect on cell proliferation was also observed using immunofluorescence for ki67, a well-known marker of cycling cells (Fig. 5B and C).

Argyrophilic nucleolar organizer region (AgNORs) morphometric analysis showed that ribosomal biogenesis (mean na/Na ratio) was significantly increased in PASMCs after PDGF stimulation; on the contrary, after HDACi treatment, it decreased and became comparable to that seen in control cells (Fig. 6A and B). A concomitant TUNEL assay showed that apoptosis was not triggered by PDGF PASMCs stimulation with or without HDACis treatment compared to control quiescent cells (data not shown).

Likewise MC1855, wound healing assay showed that HDAC1-I reduced in a dose dependent manner PDGF-induced migration in PAH-PASMCs (Fig. 6C).

Similarly to MC1855 and to HDAC1 siRNA, after a 7-h treatment HDAC1-I had a significant effect on reduction of Akt phosphorylation (Fig. 7A).

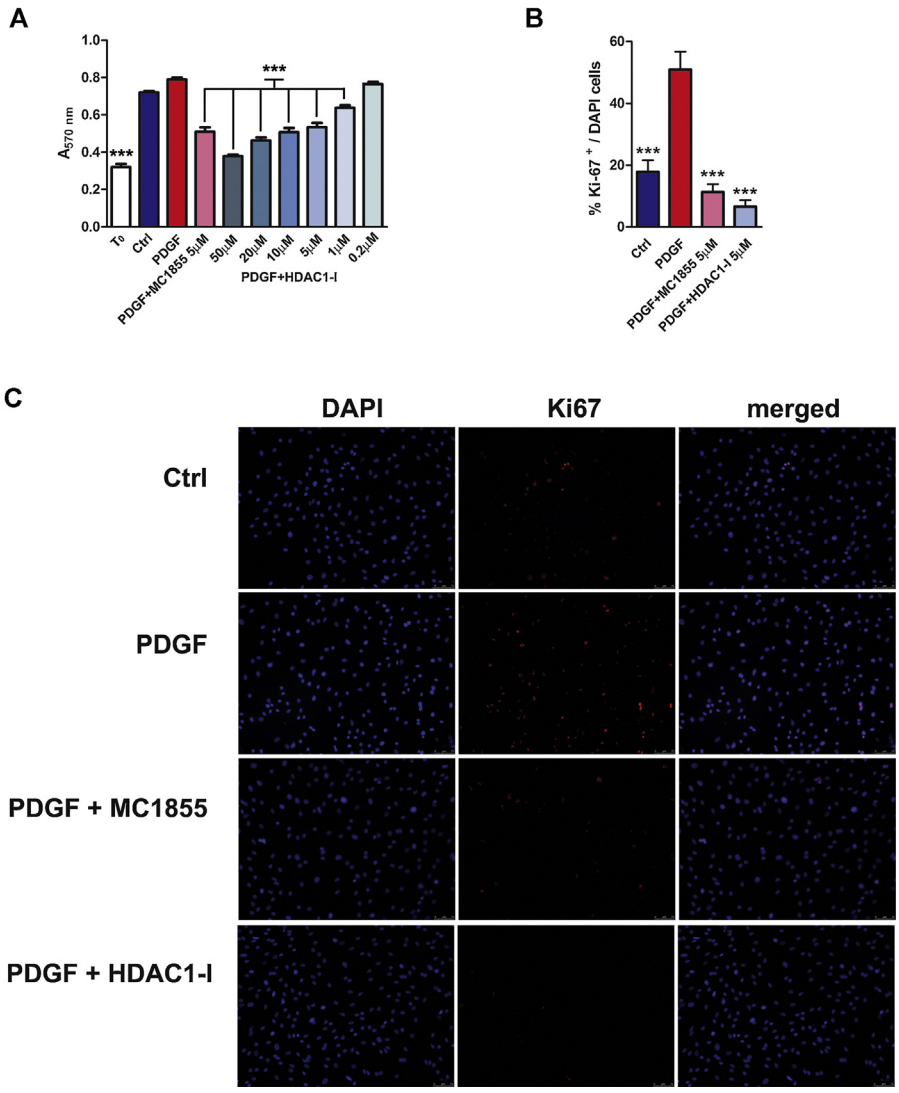

Fig. 5. Effect of HDAC1 specific inhibitor (HDAC1-I) on PDGF-induced proliferation. (A) Different doses of HDAC1-I effects on PDGF-induced proliferation evaluated by MTT assay after 24 h. (B) Percentage of cells expressing proliferation marker ki67. The quantitative results are expressed as mean ± sem and represent data averaged from 5 independent experiments $^{*}p < 0.05$; $^{**}p < 0.01$; $^{***}p < 0.005$ vs PDGF-treated group. (C) Representative images of ki67 immunostaining (red). Nuclear labeling with DAPI (blue) were used to assess total cell number. (For interpretation of the references to color in this figure legend, the reader is referred to the web version of this article.)

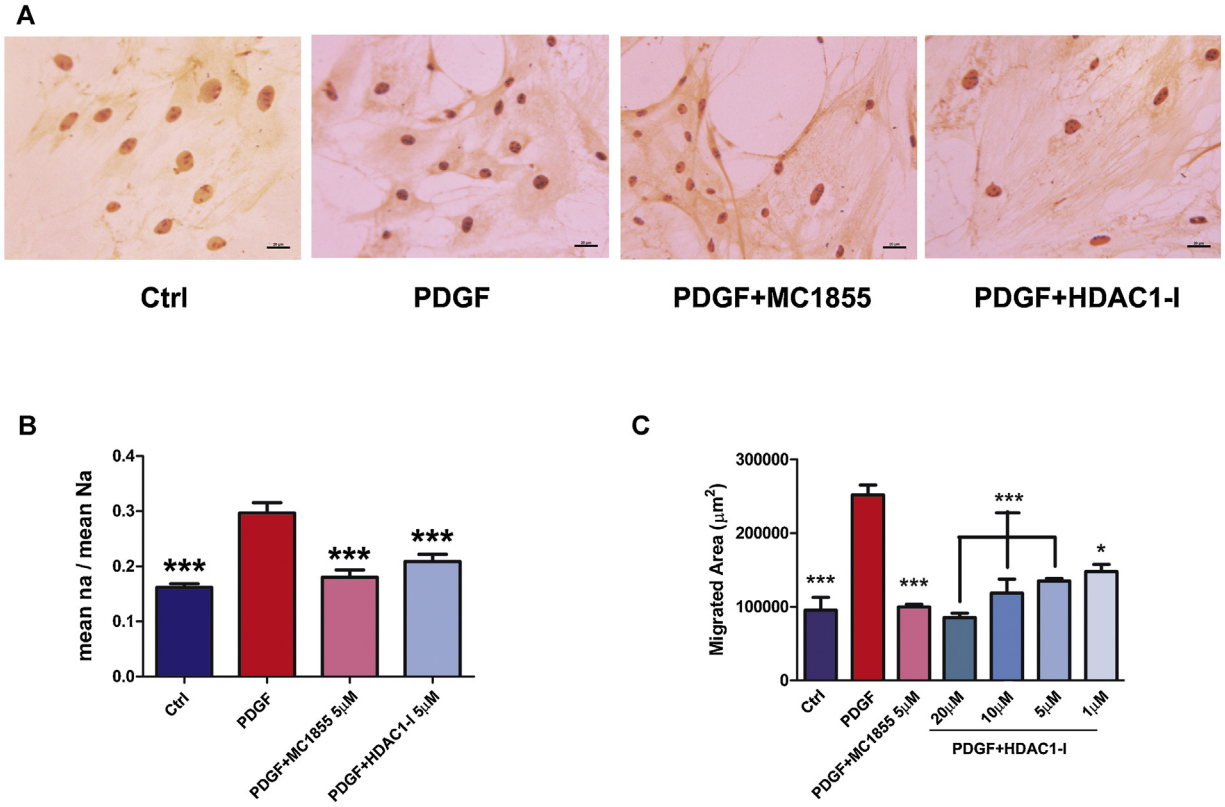

Fig. 6. Effect of HDAC1 specific inhibitor (HDAC1-I) on PDGF-induced PASMC proliferation and migration. (A) Representative images of silver-stained NOR proteins results. Scale bars: 50 μm. (B) Morphometric analysis of silver-stained NOR proteins. Results were expressed as mean nucleolar/nuclear areas (m na/m Na) ratio normalized to control. $^{***}p < 0.005$. (C) Effect of different doses of HDAC1-I on PDGF-induced migration extent, measured as the difference in cells covered area after 6 h of observation. Results from 4 different experiments are expressed as mean ± sem $^{*}p < 0.05$; $^{**}p < 0.01$; $^{***}p < 0.005$ vs PDGF treated group.

Interestingly, at the same time point HDAC1-I reduced CycD1 expression at both protein (Fig. 7A and B) and RNA (Fig. 7C) level with a stronger effect than MC1855.

4. Discussion

There is consensus evidence that an overexpression of HDACs can cause epigenetic alterations associated with malignant cell behavior, as shown by the correlation between the occurrence of many cancers and genome-wide histone hypoacetylation [29]. Very recently, Zhao et al. [11] described changes in the expression of HDAC proteins, specifically an increase in HDAC1 (class I) and HDAC5 (class II), in human IPAH lungs. Therefore, not only all cancer patients, but also PAH patients could potentially benefit from an epigenetic therapy.

We have previously tested the ability of NaBU and trichostatin A (TSA), two broad-spectrum HDACis, to counteract PDGF in inducing the proliferation of PASMCs isolated from PAH-rats [20].

Here, PASMC exposure to MC1855 and MC1575 was exploited to take a glimpse on the action of HDAC class I and/or II, respectively, in our experimental model. Naldi et al. [21] previously, demonstrated that MC1855 has an inhibitory profile similar to that of MS-275 (Entinostat), a class I HDACi [30–33], affecting hyperacetylation of all histones in HT29 colon cancer cells more potently and with lower toxicity than suberoylanilide hydroxamic acid (SAHA) a non-selective HDACi. Although the newly designed synthetic inhibitor of class II HDACs MC1575 showed to be less potent in inhibiting HDACs than pan-inhibitor TSA, it blocked dose-dependently the proliferation and induced cell cycle arrest in ERα-positive MCF-7 breast cancer cells [8] and melanoma cells [34].

Here, we show that MC1855 dose- and time-dependently inhibited proliferation and migration induced by PDGF in PASMCs isolated from PAH-rats, as well as PDGF-induced vessel sprouting from the pulmonary artery of PAH animals. The possibility that MC1855 may have acted only on class I HDAC is strongly supported by the observation that (i) the class II inhibitor MC1575 only blocked the proliferative effect of the growth factor at a concentration at which it has been shown to lack specificity for class II HDAC, also acting on class I HDAC [8], and (ii) in contrast to MC1855, MC1575 had no effect on PDGF-induced migration in PAH-PASMCs and PDGF-induced sprouting in pulmonary artery of PAH animals.

Time-course analysis of Akt phosphorylation and the results yielded in the presence of the phosphatase inhibitor CA strongly suggest that phosphatase-mediated dephosphorylation of Akt may be a major underlying mechanism of HDACi action [20].

To this end, mimicking a pan-HDACi, MC1855 decreased Akt phosphorylation at Ser473 induced by PDGF only after 7 h of treatment. In agreement with our previous data, these results suggest that HDAC inhibition may have blocked HDAC–phosphatase interaction(s), thus promoting the release of the phosphatase and its subsequent association with Akt. This hypothesis is consonant with the observation that in human glioblastoma cells HDACis can interrupt Protein Phosphatase 1 (PP1) coupling with HDAC1/HDAC6, promoting PP1/Akt assembly which leads to inhibition of kinase activity [22]. Akin to this picture, Akt deacetylation has been found to boost its phosphorylation and activation [16].

Moreover, here we demonstrated that MC1855 reduced CycD1 expression at gene and protein level. The ability of the phosphatase inhibitor CA to rescue CycD1 level suggested that Akt dephosphorylation induced by NaBU and by the class I specific HDACi is

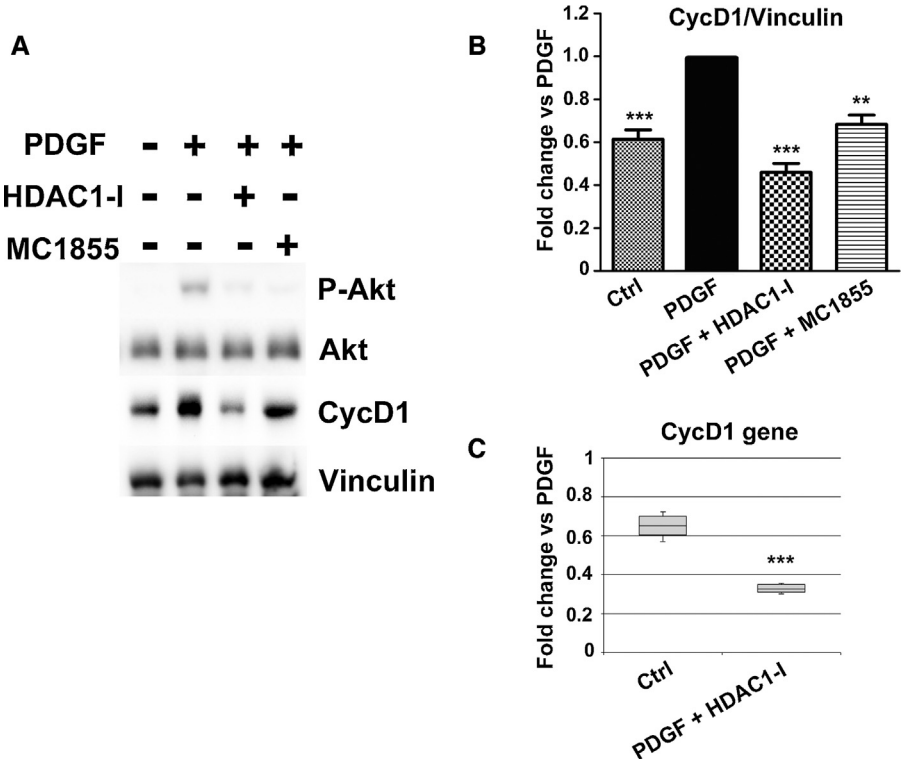

Fig. 7. Effect of HDAC1 specific inhibitor (HDAC1-I) on Akt phosphorylation and CycD1 expression. (A) Phosphorylation state of Ser473-Akt and CycD1 protein level in PASMCs after a 7 h treatment with PDGF with or without 5 μM MC1855, 5 μM HDAC1-I. Untreated cells were used as a control (Ctrl). Representative images of 5 different experiments. (B) Effect on CycD1 level as assessed by a densitometric analysis of Western blot experiments. Results were expressed as CycD1/Vinculin level change compared to that of the PDGF alone. Relative protein level quantification was shown as mean ± sem $^{**}p < 0.01$; $^{***}p < 0.005$ vs PDGF treated group. (C) Transcriptional level of CycD1 in PASMCs after 7 h PDGF-treatment with or without 5 μM HDAC1-I. Real-time PCR data, normalized to gapdh and actin b housekeeping genes, were expressed as relative fold change of PDGF + HDACi compared to PDGF alone. Results of 3 different experiments were analyzed using REST 2009 software (QIAGEN): $^{*}p < 0.05$.

tightly connected to a reduction in the amount of active (phosphorylated) protein involved in positive regulation of cell cycle.

On the contrary, the inhibition of class II HDACs failed to affect either the phosphorylation state of Akt or CycD1 level, further supporting a major involvement of class I HDACs in PDGF-induced PASMC proliferation.

Additional information on the mechanism(s) by which different HDACs belonging class I may regulate Akt phosphorylation have been obtained by transducing PASMCs with siRNA specific for each of the class I members: HDAC1, HDAC2, HDAC3 and HDAC8. Our data showed that at 7 h, a time point at which MC1855 elicited a significant downregulation of phosphorylated Akt, only HDAC1 and HDAC2 siRNA significantly reduced PDGF-induced Akt stimulation. Interestingly, siRNA against HDAC1 and HDAC2 reduced both proliferation and migration induced by PDGF treatment. However, HDAC1 siRNA reduced significantly CycD1 protein expression, highlighting the prominent role of HDAC1 in PASMC proliferation induced by PDGF. This finding is consistent whit HDAC1 overexpression previously detected in lungs from both IPAH patients and pulmonary hypertensive rats [11].

Further cue on the mechanisms underlying the action of MC1855 can be inferred by the results yielded in the presence of HDAC1-I, a commercially available HDAC1 specific inhibitor [27,28]. Remarkably, MC1855 proved to act with a similar profile to, and at the same concentration of HDAC1-I, in affecting both proliferation and migration of PASMCs.

So far, a major limitation in the therapeutic exploitation of HDACi has emerged from the conflicting results yielded by the merging of opposite effects elicited by inhibiting different isoforms of different classes at the same time [35]. The present findings highlight a selective involvement of HDAC1 within the class I of HDACs in driving a number of crucial signaling events behind the PDGF induced patterning in PAH PASMCs. Accordingly, the development of novel inhibitors selectively targeted against class I HDAC1 should be envisioned as a potentially effective tool to handle the dysfunctional behavior of PASMCs in PAH. Further studies are in progress to address this issue in in vivo PAH models.

Authors' contributions

MG: Study conception and design, Acquisition, analysis and interpretation of data. SC: Study conception and design, Acquisition, analysis and interpretation of data, Drafting and revision of the work for intellectual content and context, Final approval and overall responsibility for the published work. FZ: Acquisition, analysis and interpretation of data. SV: Acquisition, analysis and interpretation of data. MP: Acquisition, analysis and interpretation of data. AM: Analysis and interpretation of data. GP: Analysis and interpretation of data. AM: Revision of the work for intellectual content and context. NG: Final approval and overall responsibility for the published work. CV: Revision of the work for intellectual content and context; Final approval and overall responsibility for the published work.

Acknowledgements

Bayer Pharma AG, Berlin, Germany; Tavola Valdese, Rome, Italy.

References

[1] Voelkel NF, Gomez-Arroyo J, Abbate A, Bogaard HJ, Nicolls MR. Pathobiology of pulmonary arterial hypertension and right ventricular failure. Eur Respir J 2012;40:1555–65.

[2] Rabinovitch M. Molecular pathogenesis of pulmonary arterial hypertension. J Clin Invest 2012;122:4306–13.
[3] Sakao S, Tatsumi K, Voelkel NF. Reversible or irreversible remodeling in pulmonary arterial hypertension. Am J Respir Cell Mol Biol 2010;43:629–34.
[4] Schermuly RT, Dony E, Ghofrani HA, Pullamsetti S, Savai R, Roth M, et al. Reversal of experimental pulmonary hypertension by PDGF inhibition. J Clin Invest 2005;115:2811–21.
[5] Perros F, Montani D, Dorfmüller P, Durand-Gasselin I, Tcherakian C, Le Pavec J, et al. Platelet-derived growth factor expression and function in idiopathic pulmonary arterial hypertension. Am J Respir Crit Care Med 2008;178:81–8.
[6] Galiè N, Palazzini M, Manes A. Pulmonary arterial hypertension: from the kingdom of the near-dead to multiple clinical trial meta-analyses. Eur Heart J 2010;31:2080–6.
[7] Yang XJ, Seto E. HATs and HDACs: from structure, function and regulation to novel strategies for therapy and prevention. Oncogene 2007;26:5310–8.
[8] Duong V, Bret C, Altucci L, Mai A, Duraffourd C, Loubersac J, et al. Specific activity of class II histone deacetylases in human breast cancer cells. Mol Cancer Res 2008;6:1908–19.
[9] Gregoretti IV, Lee YM, Goodson HV. Molecular evolution of the histone deacetylase family: functional implications of phylogenetic analysis. J Mol Biol 2004;338:17–31.
[10] Archer SY, Meng S, Shei A, Hodin RA. p21(WAF1) is required for butyrate-mediated growth inhibition of human colon cancer cells. Proc Natl Acad Sci USA 1998;95:6791–6.
[11] Zhao L, Chen CN, Hajji N, Oliver E, Cotroneo E, Wharton J, et al. Histone deacetylation inhibition in pulmonary hypertension: therapeutic potential of valproic acid and suberoylanilide hydroxamic acid. Circulation 2012;126:455–67.
[12] Noh H, Oh EY, Seo JY, Yu MR, Kim YO, Ha H, et al. Histone deacetylase-2 is a key regulator of diabetes- and transforming growth factor-beta1-induced renal injury. Am J Physiol Renal Physiol 2009;297:F729–39.
[13] White AO, Wood MA. Does stress remove the HDAC brakes for the formation and persistence of long-term memory? Neurobiol Learn Mem 2013.
[14] Harrison IF, Dexter DT. Epigenetic targeting of histone deacetylase: therapeutic potential in Parkinson's disease. Pharmacol Ther 2013;140:34–52.
[15] Hawtree S, Muthana M, Wilson AG. The role of histone deacetylases in rheumatoid arthritis fibroblast-like synoviocytes. Biochem Soc Trans 2013;41:783–8.
[16] Minucci S, Pelicci PG. Histone deacetylase inhibitors and the promise of epigenetic (and more) treatments for cancer. Nat Rev Cancer 2006;6:38–51.
[17] Cavasin MA, Demos-Davies K, Horn TR, Walker LA, Lemon DD, Birdsey N, et al. Selective class I histone deacetylase inhibition suppresses hypoxia-induced cardiopulmonary remodeling through an antiproliferative mechanism. Circ Res 2012;110:739–48.
[18] Trivedi CM, Luo Y, Yin Z, Zhang M, Zhu W, Wang T, et al. Hdac2 regulates the cardiac hypertrophic response by modulating Gsk3 beta activity. Nat Med 2007;13:324–31.
[19] Montgomery RL, Davis CA, Potthoff MJ, Haberland M, Fielitz J, Qi X, et al. Histone deacetylases 1 and 2 redundantly regulate cardiac morphogenesis, growth, and contractility. Genes Dev 2007;21:1790–802.
[20] Cantoni S, Galletti M, Zambelli F, Valente S, Ponti F, Tassinari R, et al. Sodium butyrate inhibits platelet-derived growth factor-induced proliferation and migration in pulmonary artery smooth muscle cells through Akt inhibition. FEBS J 2013;280:2042–55.
[21] Naldi M, Calonghi N, Masotti L, Parolin C, Valente S, Mai A, et al. Histone post-translational modifications by HPLC-ESI-MS after HT29 cell treatment with histone deacetylase inhibitors. Proteomics 2009;9:5437–45.
[22] Shimoda LA, Sylvester JT, Sham JS. Mobilization of intracellular Ca(2+) by endothelin-1 in rat intrapulmonary arterial smooth muscle cells. Am J Physiol Lung Cell Mol Physiol 2000;278:L157–64.
[23] Mai A, Massa S, Pezzi R, Rotili D, Loidl P, Brosch G. Discovery of (aryloxopropenyl)pyrrolyl hydroxyamides as selective inhibitors of class IIa histone deacetylase homologue HD1-A. J Med Chem 2003;46:4826–9.
[24] Montanaro L, Govoni M, Orrico C, Treré D, Derenzini M. Location of rRNA transcription to the nucleolar components: disappearance of the fibrillar centers in nucleoli of regenerating rat hepatocytes. Cell Struct Funct 2011;36:49–56.
[25] Diehl JA, Cheng M, Roussel MF, Sherr CJ. Glycogen synthase kinase-3beta regulates Cyclin D1 proteolysis and subcellular localization. Genes Dev 1998;12:3499–511.
[26] Diehl JA, Zindy F, Sherr CJ. Inhibition of Cyclin D1 phosphorylation on threonine-286 prevents its rapid degradation via the ubiquitin-proteasome pathway. Genes Dev 1997;11:957–72.
[27] Jung M, Brosch G, Kölle D, Scherf H, Gerhäuser C, Loidl P. Amide analogues of trichostatin A as inhibitors of histone deacetylase and inducers of terminal cell differentiation. J Med Chem 1999;42:4669–79.
[28] Schmidt K, Gust R, Jung M. Inhibitors of histone deacetylase suppress the growth of MCF-7 breast cancer cells. Arch Pharm (Weinheim) 1999;332:353–7.
[29] Mai A, Massa S, Rotili D, Cerbara I, Valente S, Pezzi R, et al. Histone deacetylation in epigenetics: an attractive target for anticancer therapy. Med Res Rev 2005;25:261–309.
[30] Saito A, Yamashita T, Mariko Y, Nosaka Y, Tsuchiya K, Ando T, et al. A synthetic inhibitor of histone deacetylase, MS-27-275, with marked in vivo antitumor activity against human tumors. Proc Natl Acad Sci USA 1999;96:4592–7.
[31] Rosato RR, Almenara JA, Grant S. The histone deacetylase inhibitor MS-275 promotes differentiation or apoptosis in human leukemia cells through a process regulated by generation of reactive oxygen species and induction of p21CIP1/WAF1 1. Cancer Res 2003;63:3637–45.
[32] Hu E, Dul E, Sung CM, Chen Z, Kirkpatrick R, Zhang GF, et al. Identification of novel isoform-selective inhibitors within class I histone deacetylases. J Pharmacol Exp Ther 2003;307:720–8.
[33] Hess-Stumpp H, Bracker TU, Henderson D, Politz O. MS-275, a potent orally available inhibitor of histone deacetylases – the development of an anticancer agent. Int J Biochem Cell Biol 2007;39:1388–405.
[34] Venza I, Visalli M, Oteri R, Cucinotta M, Teti D, Venza M. Class II-specific histone deacetylase inhibitors MC1568 and MC1575 suppress IL-8 expression in human melanoma cells. Pigment Cell Melanoma Res 2013;26:193–204.
[35] Gopal YN, Arora TS, Van Dyke MW. Parthenolide specifically depletes histone deacetylase 1 protein and induces cell death through ataxia telangiectasia mutated. Chem Biol 2007;14:813–23.